

---

# Heterogeneous Substructuring Methods for Coupled Surface and Subsurface Flow

Heiko Berninger<sup>1</sup>, Ralf Kornhuber<sup>2</sup>, and Oliver Sander<sup>2</sup>

<sup>1</sup> Université de Genève, Section de Mathématiques, Switzerland,

[Heiko.Berninger@unige.ch](mailto:Heiko.Berninger@unige.ch)

<sup>2</sup> Freie Universität Berlin, Institut für Mathematik, Germany,

{kornhuber|sander}@math.fu-berlin.de

## 1 Introduction

The exchange of ground- and surface water plays a crucial role in a variety of practically relevant processes ranging from flood protection measures to preservation of ecosystem health in natural and human-impacted water resources systems.

Commonly accepted models are based on the shallow water equations for overland flow and the Richards equation for saturated–unsaturated subsurface flow with suitable coupling conditions. Continuity of mass flow across the interface is natural, because it directly follows from mass conservation. Continuity of pressure is typically imposed for simplicity. Mathematically, this makes sense for sufficiently smooth height of surface water as occurring, e.g., in filtration processes [9, 14]. Here we impose Robin-type coupling conditions modelling a thin, nearly impermeable layer at the bottom of the river bed that may cause pressure discontinuities; an effect which is known in hydrology as clogging (see [16] or [8, p. 1376]). From a mathematical perspective, clogging can be regarded as a kind of regularization, because, in contrast to Dirichlet conditions, Robin conditions can be straightforwardly formulated in a weak sense.

Existence and uniqueness results for the Richards equation and the shallow water equations are rare and hard to obtain, and nothing seems to be known about solvability of coupled problems. Extending the general framework of heterogeneous Steklov–Poincaré formulations and iterative substructuring [10, 13] to time-dependent problems, we introduce a Robin–Neumann iteration for the continuous coupled problem and motivate its feasibility by well-known existence results for the linear case. As surface and subsurface flow are only weakly coupled by clogging and continuity of mass flux, different discretizations with different time steps and different meshes can be used in a natural way. This is absolutely necessary, to resolve the vastly different time and length scales of surface and subsurface flow. Discrete mass conservation can be proved in a straightforward way.

Finally, we illustrate our considerations by coupling a finite element discretization of the Richards equation based on Kirchhoff transformation [4] with a simple

upwind discretization of surface flow. Numerical experiments confirm discrete mass conservation and show fast convergence of the Robin–Neumann iteration for real-life soil data.

## 2 Coupled Surface and Subsurface Flow

Saturated–unsaturated subsurface flow during a time interval  $(0, T_{\text{end}})$  in a porous medium occupying a bounded domain  $\Omega \subset \mathbb{R}^d$ ,  $d = 2, 3$ , is described by the Richards equation

$$n\theta(p)_t + \operatorname{div} \mathbf{v}(p) = 0, \quad \mathbf{v}(p) = -\frac{K}{\mu} kr(\theta(p)) \nabla(p - \rho g z). \quad (1)$$

The porosity  $n$ , permeability  $K$ , viscosity  $\mu$ , and density  $\rho$  are given parameters, and  $g$  is the earth’s gravitational acceleration. The unknown capillary pressure  $p$  is related to saturation  $\theta(p)$  and relative permeability  $kr(\theta(p))$  by equations of state [6, 7]

$$\theta(p) = \begin{cases} \theta_m + (\theta_M - \theta_m) \left(\frac{p}{p_b}\right)^{-\lambda} & \text{for } p \leq p_b \\ \theta_M & \text{for } p \geq p_b \end{cases}$$

$$kr(\theta) = \left(\frac{\theta - \theta_m}{\theta_M - \theta_m}\right)^{3 + \frac{2}{\lambda}}, \quad \theta \in [\theta_m, \theta_M] \subset [0, 1],$$

with residual saturation  $\theta_m$ , maximal saturation  $\theta_M$ , bubbling pressure  $p_b < 0$ , and pore size distribution factor  $\lambda > 0$ . Let  $\Gamma \subset \partial\Omega$  denote the coupling boundary of the porous medium with a surface flow, and denote the outward normal vector of  $\Gamma$  by  $\mathbf{n}$ . We impose the coupling by Robin conditions  $p|_{\Gamma} - \alpha \mathbf{v} \cdot \mathbf{n} \in L^2((0, T_{\text{end}}), H^{-1/2}(\Gamma))$  on  $\Gamma$  and homogeneous Neumann conditions on  $\partial\Omega \setminus \Gamma$ . With compatible initial conditions  $\theta_0 \in L^1(\Omega)$  we assume that (1) admits a unique weak solution  $p \in L^2((0, T_{\text{end}}), H^1(\Omega))$ . This assumption is motivated by known existence results [1] for the Kirchhoff transformed Richards equation (see also [4]) and is, obviously, satisfied in the case of saturated flow  $\theta \equiv \theta_M$ .

The surface flow on  $\Gamma$  is described by the shallow water equations

$$h_t + \operatorname{div} \mathbf{q} = r, \quad (2a)$$

$$\mathbf{q}_t + \operatorname{div} \mathbf{F}(h, \mathbf{q}) = -gh \nabla \phi \quad (2b)$$

where  $\phi : \Gamma_0 \rightarrow \Gamma$  is a parametrization of the surface topography of  $\Gamma$ . The unknown water height  $h$  and discharge  $\mathbf{q}$ , as well as a given mass source  $r$  are functions on  $(0, T_{\text{end}}) \times \Gamma_0$ . For ease of presentation, we assume  $\Gamma = \Gamma_0$  so that  $\Gamma$  is an open subset of  $\mathbb{R}^{d-1}$ . For  $d = 3$ , i.e.,  $\Gamma \subset \mathbb{R}^2$ , the flux function  $\mathbf{F}$  takes the form

$$\mathbf{F} = \begin{pmatrix} \mathbf{F}_1 \\ \mathbf{F}_2 \end{pmatrix}, \quad \mathbf{F}_1(h, \mathbf{q}) = \begin{pmatrix} q_1^2/h + \frac{1}{2}gh^2 \\ q_1q_2/h \end{pmatrix}, \quad \mathbf{F}_2(h, \mathbf{q}) = \begin{pmatrix} q_1q_2/h \\ q_2^2/h + \frac{1}{2}gh^2 \end{pmatrix}$$

with  $\mathbf{q} = (q_1, q_2)$ . It degenerates to  $\mathbf{F}(h, \mathbf{q}) = \mathbf{q}^2/h + \frac{1}{2}gh^2$  for  $\Gamma \subset \mathbb{R}$ . For suitable initial conditions and inflow conditions on  $\partial\Gamma_{\text{in}} \subset \partial\Gamma$  we assume that (2) has a weak solution  $(h, \mathbf{q}) \in L^\infty((0, T_{\text{end}}), L^\infty(\Gamma))^d$  in the sense of distributions  $\mathcal{D}'((0, T_{\text{end}}) \times \Gamma_{\text{in}})$  where  $\Gamma_{\text{in}} = \Gamma \cup \partial\Gamma_{\text{in}}$ . Since regularity results for nonlinear hyperbolic systems (2) do not seem to be available we note that this assumption is satisfied in the linear case [15, Theorem 2.2].

Mass conservation provides the Neumann coupling condition

$$r = \mathbf{v} \cdot \mathbf{n} .$$

Following, e.g. [16], we postulate a nearly impermeable river bed with thickness  $\varepsilon \ll 1$  and permeability  $K_\varepsilon$  (clogging). Then Darcy's law provides the flux  $\mathbf{v} = -\frac{K_\varepsilon}{\mu} \nabla p_\varepsilon$ . Setting  $\nabla p_\varepsilon = \varepsilon^{-1}(\rho gh - p|_\Gamma)\mathbf{n}$ , we obtain the Robin coupling condition

$$p|_\Gamma - \alpha \mathbf{v} \cdot \mathbf{n} = \rho gh \tag{3}$$

with leakage coefficient  $\alpha = \frac{\mu\varepsilon}{K_\varepsilon}$ . Note that (3) generally implies a pressure discontinuity across the interface  $\Gamma$  between ground and surface water.

*Remark 1.* In light of the above regularity assumptions on pressure  $p$  and surface water height  $h$  coupling surface and subsurface flow by continuity  $p|_\Gamma = \rho gh$  of capillary and hydrostatic pressure is generally not possible, because there is a regularity gap between the trace  $p|_\Gamma \in L^2((0, T_{\text{end}}), H^{1/2}(\Gamma))$  and  $h \in L^\infty((0, T_{\text{end}}), L^\infty(\Gamma)) \not\subset L^2((0, T_{\text{end}}), H^{1/2}(\Gamma))$  (see, e.g., [5, p. 148]) However, sufficient smoothness is available in special cases like, e.g., in- and exfiltration processes [14].

### 3 Steklov–Poincaré Formulation and Substructuring

We introduce the Robin-to-Neumann map

$$S_\Omega(h) = \mathbf{v}(h) \cdot \mathbf{n} = \alpha^{-1}(p|_\Gamma - \rho gh)$$

for  $h \in L^\infty((0, T_{\text{end}}), L^\infty(\Gamma)) \subset L^2((0, T_{\text{end}}), H^{-1/2}(\Gamma))$ . Here,  $p$  is the solution of the Richards equation (1) with Robin conditions (3). Assuming that for given  $h \in L^\infty((0, T_{\text{end}}), L^\infty(\Gamma))$  and corresponding inflow boundary conditions, the second part (2b) of the shallow water equations has a unique weak solution  $\mathbf{q}(h) \in L^\infty((0, T_{\text{end}}), L^\infty(\Gamma))^{d-1}$ , we set

$$S_\Gamma(h) = -\text{div } \mathbf{q}(h) .$$

The Steklov–Poincaré formulation of the coupled Richards equation and shallow water equations then reads

$$h_t = S_\Omega(h) + S_\Gamma(h) . \tag{4}$$

Just as (2a) and (4) is understood in the sense of distributions  $\mathcal{D}'((0, T_{\text{end}}) \times \Gamma_{\text{in}})$ .

In complete analogy to the stationary case [10, 13] we introduce a damped Robin–Neumann iteration

$$h_t^{v+1/2} - S_\Gamma(h^{v+1/2}) = S_\Omega(h^v), \quad h^{v+1} = h^v + \omega(h^{v+1/2} - h^v), \quad (5)$$

with a suitable damping parameter  $\omega \in (0, \infty)$  and with an initial iterate given by  $h^0 \in L^\infty((0, T_{\text{end}}), L^\infty(\Gamma))$ . Each step amounts to the solution of the Richards equation with Robin boundary conditions (3) to evaluate the source term  $S_\Omega(h^v)$ , and the subsequent solution of the shallow water equations (2) to evaluate  $h^{v+1/2}$ . The feasibility of (5) requires existence and uniqueness of these solutions. Note the similarity to waveform relaxation methods [11].

After selecting a step size  $\Delta T = T_{\text{end}}/N$  with suitable  $N \in \mathbb{N}$  and corresponding time levels  $T_k = k\Delta T$ , the Robin–Neumann iteration (5) can also be applied on subintervals  $[T_{k-1}, T_k]$ ,  $k = 1, \dots, N$ .

## 4 Discretization and Discrete Robin–Neumann Iteration

We first derive a discrete version of the Steklov–Poincaré formulation (4) on a fixed time interval  $[T_k, T_{k+1}]$  with  $0 \leq T_k < T_{k+1} = T_k + \Delta T \leq T_{\text{end}}$ . To this end, we introduce intermediate time levels  $t_i = T_k + i\tau$ ,  $i = 0, \dots, M$ , with step size  $\tau = \Delta T/M$  and suitable  $M \in \mathbb{N}$ . Spatial discretization is based on a partition  $\mathcal{T}_\Gamma$  of  $\Gamma$  into simplices  $T$  that is regular in the sense that the intersection of two simplices  $T, T' \in \mathcal{T}_\Gamma$  is either a common face, edge, vertex, or empty. We introduce the corresponding space of discontinuous finite elements of order  $q \geq 0$  by

$$\mathcal{V}_\Gamma = \{v \in L^2(\Gamma) \mid v_T \text{ is a polynomial of degree at most } q \forall T \in \mathcal{T}_\Gamma\},$$

and let  $h = (h_i)_{i=0}^M$  denote approximations  $h_i \in \mathcal{V}_\Gamma$  at  $t_i$ ,  $i = 0, \dots, M$ .

Then, utilizing the forward difference quotient  $\partial_t h_i = (h_{i+1} - h_i)/\tau$ , a discrete Steklov–Poincaré formulation reads

$$\partial_t h_i = S_\Gamma(h)_i + S_\Omega(h)_i, \quad i = 0, \dots, M-1. \quad (6)$$

Here and in the rest of this section, subscripts  $i$  indicate approximations taken at time  $t_i$ .

For given  $h = (h_i)_{i=0}^M$ , the discrete surface flow

$$(S_\Gamma(h)_i, v)_\Gamma = \sum_{T \in \mathcal{T}_\Gamma} ((\mathbf{q}(h)_i, \nabla v)_T + (\mathbf{G}_h(h_i, \mathbf{q}(h)_i) \cdot \mathbf{n}_T, v)_{\partial T}) \quad \forall v \in \mathcal{V}_\Gamma \quad (7)$$

results from an explicit discontinuous Galerkin discretization of (2a), characterized by the discrete flux function  $\mathbf{G}_h$ . Here,  $(\cdot, \cdot)_U$  stands for the  $L^2$  scalar product on  $U = \Gamma, T, \partial T$ , respectively;  $\mathbf{n}_T$  is the outward normal on  $T$ , and the discrete discharge  $\mathbf{q}_i = \mathbf{q}(h)_i$  is obtained from an explicit discontinuous Galerkin discretization of (2b)

$$(\partial_t \mathbf{q}_i, v)_\Gamma = \sum_{T \in \mathcal{T}_\Gamma} ((\mathbf{F}(h_i, \mathbf{q}_i), \nabla v)_T + (\mathbf{G}_q(h_i, \mathbf{q}_i) \cdot \mathbf{n}_T, v)_{\partial T}) \quad \forall v \in (\mathcal{V}_\Gamma)^{d-1}. \quad (8)$$

Since we expect the dynamics of subsurface flow to be much slower than the surface water dynamics, we use the macro time step  $\Delta T$  for an implicit time discretization of  $S_\Omega(h)$ . The spatial discretization is based on conforming piecewise linear finite elements

$$\mathcal{V}_\Omega = \{v \in C(\overline{\Omega}) \mid v|_T \text{ is affine linear } \forall T \in \mathcal{T}_\Omega\}$$

with respect to a regular partition  $\mathcal{T}_\Omega$  of  $\Omega$ . No compatibility conditions on  $\mathcal{T}_\Omega$  and  $\mathcal{T}_\Gamma$  are required. For given  $p_k \in \mathcal{V}_\Omega$  and  $h_{k+1} \in \mathcal{V}_\Gamma$ , the discrete capillary pressure  $p_{k+1} \in \mathcal{V}_\Omega$  is then obtained from the variational equality

$$\begin{aligned} n\langle \theta_{k+1}, v \rangle_\Omega + \Delta T ((\mathbf{v}_{k+1}, \nabla v)_\Omega \\ + \alpha^{-1} (\langle p_{k+1}|_\Gamma, v \rangle_\Gamma - (\rho g h_{k+1}, v)_\Gamma)) = n\langle \theta_k, v \rangle_\Omega \quad \forall v \in \mathcal{V}_\Omega. \end{aligned} \tag{9}$$

Here  $\langle \cdot, \cdot \rangle_\Omega$  denotes the lumped  $L^2$  scalar product on  $\Omega$ ,  $\langle \cdot, \cdot \rangle_\Gamma$  is the corresponding lumped  $L^2$  scalar product on  $\Gamma$ ,  $\theta_k = \theta(p_k)$ , and  $\mathbf{v}_{k+1}$  is a discretization of the flux  $\mathbf{v}$  at  $T_{k+1}$ . Once  $p_{k+1} \in \mathcal{V}_\Omega$  is available, we set for all  $i = 0, \dots, M$

$$(S_\Omega(h)_i, v)_\Gamma = \alpha^{-1} (p_{k+1}|_\Gamma - \rho g h_{k+1}, v)_\Gamma \quad \forall v \in \mathcal{V}_\Gamma. \tag{10}$$

Note that  $S_\Omega(h)_i$  is constant on the macro interval  $[T_k, T_{k+1}]$  and only depends on  $h_{k+1}$ .

Testing (6) and (9) with constant functions  $\mathbf{1} \in \mathcal{V}_\Gamma$  and  $\mathbf{1} \in \mathcal{V}_\Omega$ , respectively, and using  $\langle p_{k+1}|_\Gamma, \mathbf{1} \rangle_\Gamma = (p_{k+1}|_\Gamma, \mathbf{1})_\Gamma$  we obtain discrete mass conservation.

**Proposition 1.** *The discrete Steklov–Poincaré formulation (6) with  $S_\Gamma$  and  $S_\Omega$  defined by (7) and (10) is mass conserving in the sense that*

$$(h_{k+1}, \mathbf{1})_\Gamma + n\langle \theta_{k+1}, \mathbf{1} \rangle_\Omega = (h_k, \mathbf{1})_\Gamma + n\langle \theta_k, \mathbf{1} \rangle_\Omega + \tau \sum_{i=0}^{M-1} (\mathbf{G}_h(h_i, \mathbf{q}_i) \cdot \mathbf{n}_{\partial\Gamma}, \mathbf{1})_{\partial\Gamma}$$

holds for  $k = 0, 1, \dots$ , with  $\mathbf{n}_{\partial\Gamma}$  denoting the outward normal on  $\partial\Gamma$ .

We emphasize that this result holds for arbitrary discretizations of the Richards flux  $\mathbf{v}$ .

The discrete Steklov–Poincaré formulation (6) gives rise to the discrete damped Robin–Neumann iteration

$$\partial_t h_i^{v+1/2} - S_\Gamma(h^{v+1/2})_i = S_\Omega(h^v)_i, \quad h_i^{v+1} = h_i^v + \omega(h_i^{v+1/2} - h_i^v), \tag{11}$$

with suitable damping parameter  $\omega \in (0, \infty)$ , and an initial iterate  $h_i^0 \in \mathcal{V}_\Gamma$  for  $i = 0, \dots, M$ . Each step amounts to the solution of the discretized Richards equation (9) to obtain  $S_\Omega(h^v)_i$  from (10) with  $p_{k+1} = p_{k+1}^v$ , and to  $M$  time steps of the discontinuous Galerkin discretization of (2) described by (7) and (8) to obtain  $h_i^{v+1/2}$ ,  $i = 1, \dots, M$ . For  $k > 0$  the initial iterate  $h^0$  is the solution of the preceding time step. We emphasize that no compatibility conditions on the different meshes  $\mathcal{T}_\Gamma$  and  $\mathcal{T}_\Omega$  are necessary, because only weak coupling conditions are involved.

## 5 Numerical Experiments

We consider a model problem on a square  $\Omega \subset \mathbb{R}^2$  of side length 10 m and select  $\Gamma$  as the upper part of its boundary. The soil parameters are  $n = 0.437$ ,  $\theta_m = 0.0458$ ,  $\theta_M = 1$ ,  $p_b = -712.2$  Pa,  $\lambda = 0.694$ , and  $K = 6.66 \cdot 10^{-9}$  m<sup>2</sup> (sandy soil). The viscosity and density of water is  $\mu = 1$  m Pa s and  $\rho = 1,000$  kg m<sup>-3</sup>, respectively. In accordance with measurements [16] we select the leakage coefficient as  $\alpha = \rho g L^{-1}$  with  $L = 10^{-6}$  s<sup>-1</sup> allowing for large pressure jumps across the interface.

We choose the initial conditions  $\theta_0 \equiv \theta(-20$  Pa) = 0.1401,  $h(0) \equiv 1$  m,  $\mathbf{q}(0) \equiv 10$  m<sup>2</sup> s<sup>-1</sup>, and inflow boundary conditions for  $h(0, t)$  and  $\mathbf{q}(0, t)$  alternating between 2 and 1 m and 20 and 10 m<sup>2</sup> s<sup>-1</sup>, respectively, with a period of 10 s. This leads to a supercritical water flow from left to right, which can result, for example, from opening a flood gate.

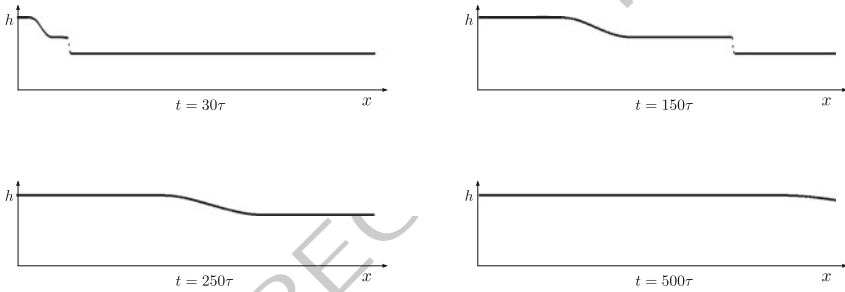


Fig. 1. The water height  $h_i$  at times  $t_i = i\tau$ ,  $i = 30, 150, 250, 500$



Fig. 2. The pressure  $p$  at times  $T_k = k\Delta T$ ,  $k = 200, 1,000, 2,000, 3,000$

For the porous media flow on  $\Omega$  we use the uniform time step size  $\Delta T = 50$  s and a triangulation  $\mathcal{T}_\Omega$  resulting from six uniform refinement steps applied to a partition of  $\Omega$  into two triangles with hypotenuse from lower left to upper right. The Richards equation (1) is discretized by the implicit scheme based on Kirchhoff transformation suggested in [4], and truncated monotone multigrid [12] is used as the algebraic solver. For the surface flow we use the time step size  $\tau = \gamma \Delta T$  with  $\gamma = 3^{-1} \cdot 10^{-4}$ ,

this figure will be printed in b/w

and the partition  $\mathcal{T}_\Gamma$  consists of 400 elements of equal length. Note that  $\mathcal{T}_\Gamma$  does not match with  $\mathcal{T}_\Omega|_\Gamma$ . The shallow water equations (2) are discretized by a discontinuous Galerkin method (7) with  $\mathcal{V}_\Gamma$  consisting of piecewise constant functions, and we use simple upwind flux functions  $\mathbf{G}_h$  and  $\mathbf{G}_q$  in (7) and (8), respectively. The final time is  $T_{\text{end}} = 3.5 \cdot 10^4$  s. For the implementation we used the DUNE libraries [2] and the domain decomposition module `dune-grid-glue` [3].

Figure 1 shows the evolution of the surface water height  $h$  over the first period of the boundary conditions. The porous medium flow is much slower, as expected. Figure 2 shows the evolution of the pressure. Water enters the domain from the top, and after about 3,600 macro time steps or, equivalently, 3,000 m, the soil saturation is constant at about 75 %. Then, the domain gets fully saturated starting from the bottom. Hydrostatic pressure builds up and is fully reached at time step 4,700.

At each time step we observe discrete mass conservation up to machine precision. The total relative mass loss over the entire evolution is about  $10^{-10}$ . Our numerical computations thus nicely reproduce the theoretical findings of Proposition 1.

In order to investigate the convergence behavior of the Robin–Neumann iteration (11), we consider the algebraic error  $\|h_M - h_M^v\|_{L^1(\Gamma)}$  at the end of the first time interval  $[0, T_1]$  with  $T_1 = M\tau$ . It turns out that for the given leakage coefficient  $\alpha = \rho g 10^6$  s (cf. [16]), the convergence rates are in the range of  $10^{-4}$ . They remain there during the entire evolution. For each time step only two or three iterations were necessary to reduce the estimated algebraic error below the threshold  $10^{-12}$ . This is explained by the weak (in the physical sense) coupling of surface water and subsurface flow associated with large values of  $\alpha$ .

The convergence speed of (11) decreases for decreasing  $\alpha$ . This is illustrated in Fig. 3 which shows convergence rates  $\rho$  of (11) for various  $\alpha$  together with the corresponding optimal damping factors  $\omega$  determined numerically. Convergence rates

this figure will be printed in b/w

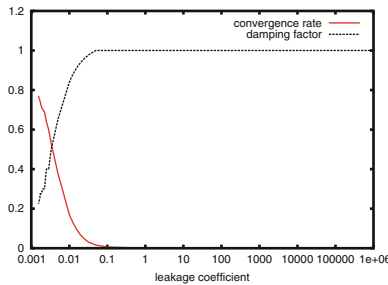


**Fig. 3.** Convergence rates  $\rho$  and associated optimal damping parameter  $\omega$  over leakage coefficient  $\alpha$

deteriorate for  $\alpha < 4 \cdot 10^{-2}$ . Moreover, for  $\alpha < 2 \cdot 10^{-3}$  ill-conditioning of the discretized Richards equation (9) leads to severe problems in the numerical solution. Hence, using the Robin coupling (3) to enforce continuity of pressure by penaliza-

tion rather than for modelling the clogging effect would require the construction of 200  
suitable preconditioners and a careful selection of  $\alpha$ . 201

## Bibliography 202

- [1] H.W. Alt and S. Luckhaus. Quasilinear elliptic–parabolic differential equations. 203  
*Math. Z.*, 183:311–341, 1983. 204
- [2] P. Bastian, M. Blatt, A. Dedner, C. Engwer, R. Klöforn, R. Kornhuber, 205  
M. Ohlberger, and O. Sander. A generic interface for parallel and adaptive 206  
scientific computing. Part II: Implementation and tests in DUNE. *Computing*, 207  
82(2–3):121–138, 2008. 208
- [3] P. Bastian, G. Buse, and O. Sander. Infrastructure for the coupling of Dune 209  
grids. In *Proc. of ENUMATH 2009*, pages 107–114. Springer, 2010. 210
- [4] H. Berninger, R. Kornhuber, and O. Sander. Fast and robust numerical solution 211  
of the Richards equation in homogeneous soil. Technical Report A /01/2010, 212  
FU Berlin, 2010. submitted to SIAM J. Numer. Anal. 213
- [5] F. Brezzi and G. Gilardi. Functional spaces. In H. Kardestuncer and D.H. 214  
Norrie, editors, *Finite Element Handbook*, chapter 2 (part 1), pages 1.29–1.75. 215  
Springer, 1987. 216
- [6] R.J. Brooks and A.T. Corey. Hydraulic properties of porous media. Technical 217  
Report Hydrology Paper No. 3, Colorado State University, 1964. 218
- [7] N.T. Burdine. Relative permeability calculations from pore-size distribution 219  
data. *Petr. Trans., Am. Inst. Mining Metall. Eng.*, 198:71–77, 1953. 220
- [8] C. Dawson. Analysis of discontinuous finite element methods for ground water 221  
/surface water coupling. *SIAM J. Numer. Anal.*, 44(4):1375–1404, 2006. 222
- [9] C. Dawson. A continuous/discontinuous Galerkin framework for modeling 223  
coupled subsurface and surface water flow. *Comput. Geosci*, 12:451–472, 2008. 224
- [10] S. Deparis, M. Discacciati, G. Fourestey, and A. Quarteroni. Fluid–structure 225  
algorithms based on Steklov–Poincaré operators. *Comput. Methods Appl. Mech.* 226  
*Engrg.*, 195:5797–5812, 2008. 227
- [11] L. Halpern. Schwarz waveform relaxation algorithms. In *Domain Decomposition 228  
Methods in Science and Engineering XVII*, volume 60 of *Lecture Notes in* 229  
*Computational Science and Engineering*, pages 155–164. Springer, 2008. 230
- [12] R. Kornhuber. On constrained Newton linearization and multigrid for varia- 231  
tional inequalities. *Numer. Math.*, 91:699–721, 2002. 232
- [13] A. Quarteroni and A. Valli. *Domain Decomposition Methods for Partial Dif-* 233  
*ferential Equations*. Oxford Science Publications, 1999. 234
- [14] P. Sochala, A. Ern, and S. Piperno. Mass conservative BDF-discontinuous 235  
Galerkin/explicit finite volume schemes for coupling subsurface and overland 236  
flows. *Comput. Methods Appl. Mech. Engrg.*, 198:2122–2136, 2009. 237
- [15] N.J. Walkington. Convergence of the discontinuous Galerkin method for dis- 238  
continuous solutions. *SIAM J. Numer. Anal.*, 42:1801–1817, 2005. 239
- [16] B. Wiese and G. Nützmann. Transient leakance and infiltration characteristics 240  
during lake bank filtration. *Ground Water*, 47(1):57–68, 2009. 241